SEMARAK ILMU PUBLISHING

Semarak International Journal of Nanotechnology

Journal homepage:
https://semarakilmu.my/index.php/sijn/index
ISSN: 3030-6604

Synthesized Hybrid CNT Polymer Composite in Reducing EMI Pollution at Gigahertz Frequency Range

Fadzidah Mohd Idris[1,*], Mohd Shamsul Ezzad Shafie, Siti Nor Ain Rusly[2], Hatika Kaco[1], Siti Munirah Mohd[1], Nurhidaya Mohamad Jan[1], Abubakar Yakubu[3]

[1] Advanced Technology and Sustainability Unit, Kolej PERMATA Insan, Universiti Sains Islam Malaysia, Bandar Baru Nilai, 71800 Nilai, Malaysia
[2] Centre for Defence Foundation Studies, National Defence University of Malaysia, Malaysia
[3] Department of Physics, Kebbi State University of Science and Technology, Aliero, Nigeria

ARTICLE INFO

Article history:
Received : 10 March 2024
Received in revised form : 28 March 2024
Accepted : 30 April 2024
Available online : 10 June 2024

Keywords:
Hybrid; carbon nanotubes; composites; reflection loss

ABSTRACT

Modern digital systems are seriously impacted by the electromagnetic (EM) danger caused by various EM wave that interfere one another, either internally or externally. The electromagnetic interference (EMI) pollution has become an attention among researchers since it not only affects the devices, but also affecting human and biological systems. Thus, synthesizing an EM wave absorber that able to absorb the unwanted EM wave signal is crucial. This research highlight on the materials' properties and characterization of the synthesized nanometer size hybrid Carbon Nanotubes (CNTs) of individual ferrite ($Ni_{0.5}Zn_{0.5}Fe_2O_4$ or Carbonyl iron) and mixed ferrite ($Ni_{0.5}Zn_{0.5}Fe_2O_4$ + Carbonyl iron) as catalyst to grow CNTs by using Chemical Vapour Deposition (CVD) method. The synthesized hybrid CNTs used as fillers were mixed with epoxy resin and hardener as the matrix at certain ratio of thickness fixed at 1 mm, 2 mm, and 3 mm. The hybrid CNTs was analysed by using X-ray diffractometer (XRD), a Field emission Scanning Electron Microscope (FeSEM) and RAMAN spectrometer to determine the phase formation, microstructural and structural analysis respectively. On the other hand, the Vector Network Analyzer (VNA) measured at 8 to 18 GHz frequency range was used to measure and analyse the microwave characterization. The phase analysis confirmed the existence of Carbon and Iron Carbide, whereas the microstructural shows the synthesized hybrid CNTs are mostly straight like, twisted and spiral fiber. Moreover, the structural analysis shows more defective structure with the formation of multiwalled CNTs that helps in absorbing the EM wave. The reflection loss (RL) of the growth individual $Ni_{0.5}Zn_{0.5}Fe_2O_4$ and Carbonyl Iron shows the RL value of -18 dB and -15 dB of thickness 2 mm respectively. The RL result also show improvement in the RL values for the growth of mixed ferrite with RL reach until -26 dB (thickness=3mm). Consequently, it indicates that using both single and mixed ferrite as a catalyst to grow CNT produces better EM wave performance appropriate for various applications.

* *Corresponding author.*
E-mail address: fadzidahmohdidris@usim.edu.my

https://doi.org/10.37934/sijn.1.1.112b

1. Introduction

The growth of higher frequency devices creates more electromagnetic interference (EMI) in life, telecommunication, industry and military. The phenomenon known as EMI is characterized as the transfer of disruptive electromagnetic radiation from one electronic device to another through either conducted or radiated routes, or both, resulting in malfunctions in the device's performance. Therefore, lightweight and thin thickness microwave absorption materials with strong absorption capability were needed to overcome the problems. Microwave absorption materials interact with either or both of these two fields to attenuate and absorb the microwaves signal that can be interpreted as a coupling of an oscillating, intergenerative electric field and magnetic field propagating in the same direction as reported by Pang *et al.,* [1]. According to research reported by Lu *et al.,* [2], the EM wave absorber works by absorbing the EM wave energy, transforming it into heat or other types of energy and finally dissipates it through attenuation and loss. This could enhance the transmission route that contributes to higher EM wave absorbers.

Binary combinations that function as active catalysts with higher activity than the individual elements are frequently used, such as nickel (Ni), iron (Fe), and cobalt (Co). Because of their special chemical, physical, and mechanical characteristics, carbon nanotubes (CNTs) are well recognized for growing from an active catalyst and may be modified to be lightweight, strong, and have a wide absorption bandwidth. Because of this, materials are always utilized in the form of mixtures and composites to balance the requirements of lightweight, high absorption, and wide absorbing bandwidth.

According to Mohamad *et al.,* [3], carbon fiber reinforced composites (CFRC) are still important for the growth and development of many different sectors that need lightweight components. They can also potentially operate as an EM wave absorber as also reported by Idris *et al.,* [4]. The conductive network created by carbon nanotubes (CNTs) experiences surface polarization and dielectric relaxation, which transform the dielectric and resistance loss of electromagnetic waves into thermal energy dissipation. This suggests the characteristics of the CNT materials' absorption type for EM wave absorption. According to Gao *et al.,* [5], CNTs have a higher capacity for EM wave absorption than other carbon-based materials because of their flexibility, less weight, thinner profile, and bigger specific surface area. Mohamad *et al.,* [3] reported that it is anticipated that adding carbon fibers to thermoplastics will enhance the mechanical, tribological, and physical characteristics of the composites.

The modification of CNTs is highlighted in this study, with a focus on their ability to absorb electromagnetic waves. Since commercial CNT is expensive, in this research CNT was synthesized by using chemical vapor deposition (CVD) method to create spiral hybrid multiwalled carbon nanotubes (MWCNTs) by combining Nickel zinc ferrite and carbonyl iron as a catalyst. Thus, by growing CNT and being incorporated into polymer matrix, it shows better improvement in absorbing performances compared to ferrite materials alone, mixed ferrite, mixed ferrite with commercial CNT. Moreover, by using this technique the sample is much lighter compared to others. Research has not been done for composite sample mixed ferrite and to be used as catalyst to grow Carbon nanotubes by using CVD method. Therefore, this research fills in the gap in examine the materials and microwave properties of synthesized MWCNTs made from mixed ferrite as a catalyst.

2. Methodology

2.1 Synthesis of Fillers

The mixture of different percentages of Carbonyl Iron and sintered Nickel Zinc Ferrite was used as catalyst to synthesize carbon nanotubes by using Chemical Vapour Deposition (CVD) method. Carbonyl iron >97% Fe basis was purchased from Sigma Aldrich. Nickel Oxide (NiO) 99.00%, Zinc Oxide (ZnO) 99.90% and Iron (III) Oxide (Fe_2O_3) 99.50% were purchased from Alfa Aesar and were mixed with certain amount according to the chemical equation to obtain $Ni_{0.5}Zn_{0.5}Fe_2O_4$ (Figure 1(a)). The $Ni_{0.5}Zn_{0.5}Fe_2O_4$ powder was mixed and milled by using high energy ball milling (HEBM) in a hardened steel vial (Figure 1(b)) together with grinding balls (Figure 1(c)) and further sintered at 900^0C for 10 hours to obtain the full phase.

The individual Carbonyl Iron (CI) and Nickel Zinc Ferrite (N) and mixture of 20% N + 80% CI (S1), 50% N + 50% CI (S2) and 80% N + 20% CI (S3) were used as catalyst and placed in a ceramic boat. The ceramic boat was then placed in the middle of the furnace. The reaction temperature was set up to 700^0C for 30 minutes. Ethanol was used as carbon source while argon gas was used as carrier gas. Figure 1 (d) shows the synthesized carbon nanotubes that were obtained.

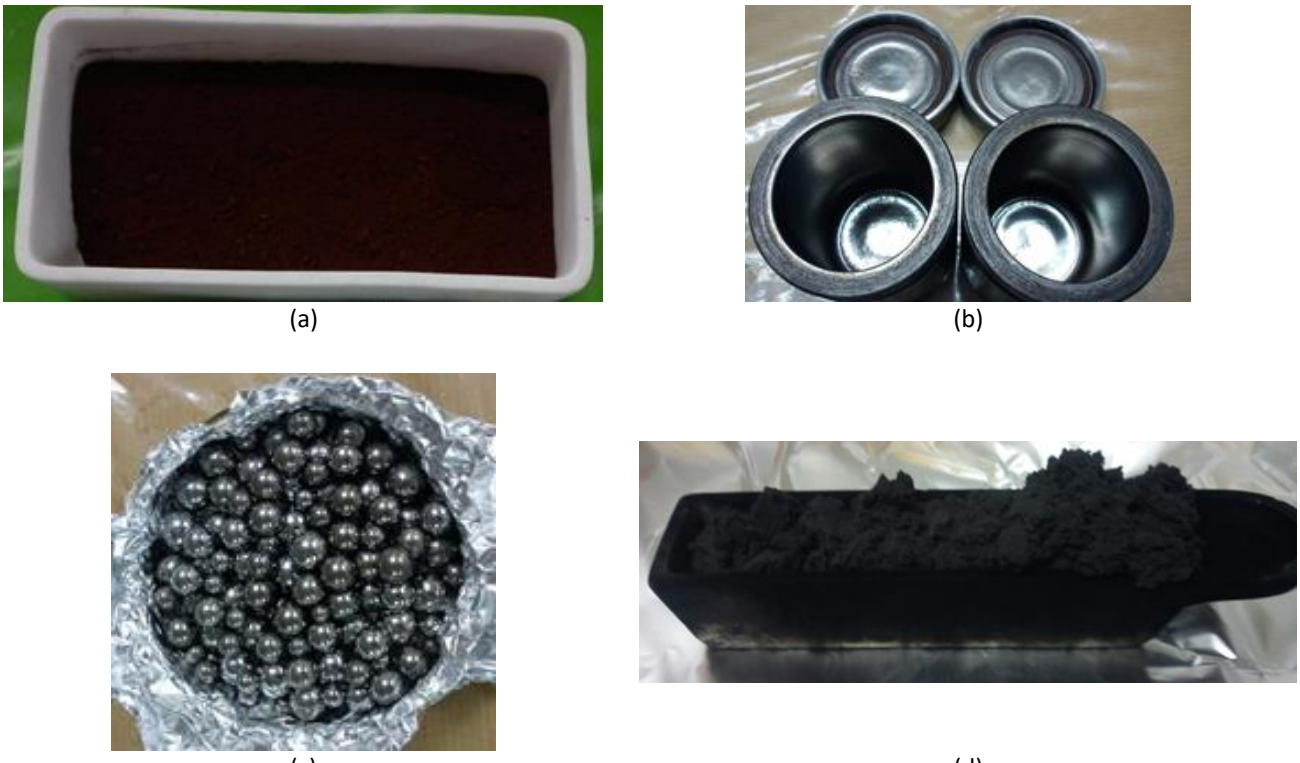

(a) (b) (c) (d)

Fig. 1. (a) sintered $Ni_{0.5}Zn_{0.5}Fe_2O_4$, (b) hardened steel vial, (c) steel ball and (d) synthesized carbon nanotubes

2.2 Synthesis of Filler-Matrix

The fillers were weighed according to the ratio of fillers being mixed with epoxy resin as a polymer matrix and the loading of fillers was fixed at 8wt%. The epoxy resin and hardener as a curing agent were added according to ratio 10:1 respectively for 15 to 20 minutes by using mini vortex mixer at 3000 rpm. Further, the homogeneous mixture was poured into the customized sample holder at different dimensions for the microwave measurement at X-band (Figure 2(a) and Ku-band (Figure 2(b)).

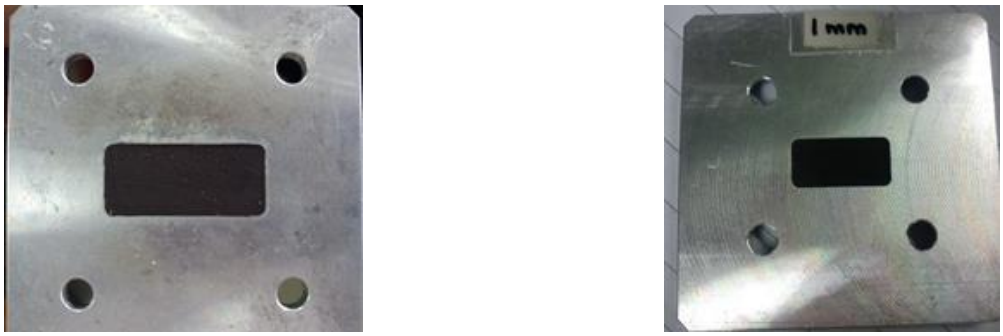

(a) (b)

Fig. 2. Sample holder at (a) X-band and (b) Ku band

2.3 Materials' Characterization

The phase analysis was carried out in the 2θ range of 20 to 80^0 by using an X-Pert PANalytical diffractometer (PW3050/60). Measurement of sample's surface morphology was measured by using a Field Emission Scanning Electron Microscope (FESEM) brand FEI NOVA. The vibrational phonon modes were identified, and further precise structural information of the carbon nanostructures were measured by using Raman spectroscopy using a WITec Alpha 300R 532 nm excitation laser. The microwave characterization of the polymer composite sample was measured by using Vector Network Analyzer (VNA) at X-band (8-12 GHz) and Ku-band (12-18 GHz) frequency range. The prepared sample was measured by using metal plate and one-port measurement to directly obtain the reflection loss or S11 parameter.

3. Results and discussion

3.1 Phase Analysis

XRD analysis was performed to investigate the microstructure evolution of different types of fillers being loaded into epoxy matrix. The XRD pattern in Figure 3 shows two main phases that consist of Carbon (G) and Iron Carbide (Fe_3C). However, there also exist three additional peaks that are assigned to the presence of catalyst in CNT as reported by Belin and Epron [6]. The main peak of carbon graphite and iron carbide were matched with the standard reference code data of 98-001-7175 and 98-009-1656 respectively. Six carbon graphite peaks presence in the sample are at 2θ angle of 26.645^0, 43.352^0, 46.016^0, 54.612^0, 56.791^0 and 77.856^0. According to several authors [7, 8], the peaks are assigned as the hexagonal graphitic phase of carbon. They were generated possibly by the reflections from basal hexagonal carbon atomic networks and by the layers of parallel nanotube stacking. The highest diffraction peak of carbon graphite indicates (002) plane. This peak shows some distinct similarities to those of graphite due to their similar intrinsic graphene properties. However, it was not identical since CNTs have different chiralities and different layers as being reported by an author [9].

The morphological orientation of CNTs determines their diffraction peak intensities, when an X-ray beam hits a single CNT wall, it creates (002) peaks. The X-ray beams create several more hexagonal peak arrays as they pass through the CNTs' empty center core. Wang and Hui [10] state that depending on the number of helices present, this may happen more than once at various azimuths. Nevertheless, majority of the carbon peak was not attainable since the CNT strains had curved graphene layers and varied sizes and shapes. This might suppress some reflection peaks, that would then cause peak shifting and broadening as reported by Tessonnier *et al.,* [11].

At the 2θ angles of 37.904^0, 40.083^0, 40.931^0, 44.079^0, 44.926^0, 49.406^0, 58.365^0, and 62.965^0, the remaining eight peaks are associated with iron carbide. Despite the presence of carbon (C) and iron (Fe) during the CVD process, the iron carbide phase formed. It was proven by McCaldin *et al.*, [12] that iron carbide formed under all conditions, irrespective of the type of CNT produced by the catalyst particle or the quantity of carbon deposited. As a result, during the synthesis process, all of the iron-based catalyst was replaced by iron carbide, which formed on the active catalytic phase. Additionally, according to McCaldin *et al.*, [12], iron oxide catalyst is eliminated by the presence of graphite and iron carbide following the CVD procedure.

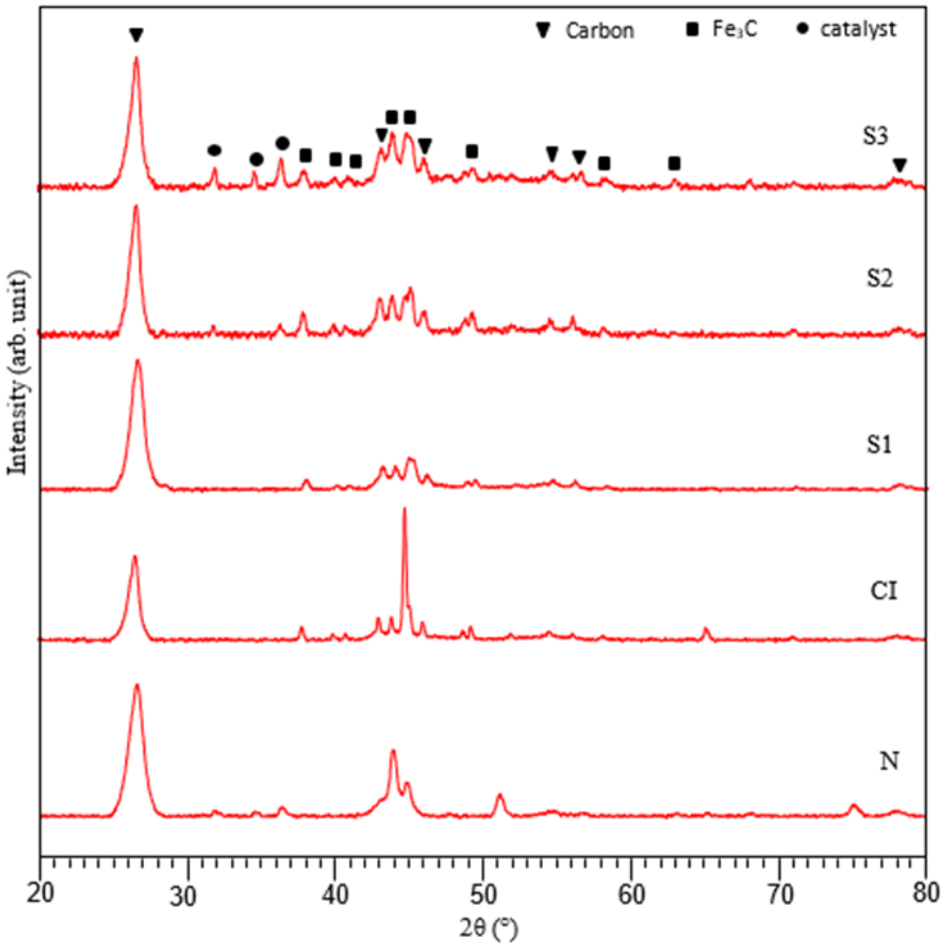

Fig. 3. X-ray diffraction pattern of different synthesized carbon nanotubes by using different catalysts

3.2 Microstructural Analysis

As the CNTs are synthesized, they naturally pull toward one another and show an increased tendency to form bundles or entanglements made up of 50 to several hundred individual CNTs due to a strong Van der Waals force. Figure 4(a) show as-synthesised CNT bundles and entanglements that are not loaded into a matrix. The most common forms of carbon structures were twisted, spiral, and straight fibers. Additionally, the tubular nature was confirmed by the presence of hollow and tube-like structures, whereas net-like fibers were generated by the aggregation of extremely tiny fibers. However, most of the fibers prefer to develop in spiral coils because of the pentagon-

heptagon pairs are regularly inserted at junctions. Furthermore, the transformation of the fibers into coils is mostly caused by the strong anisotropy of the various crystal faces of the nickel catalyst.

Fejes and Hernádi [13] discussed the mechanism of formation of coiled carbon nanotubes in detail, while Hikita *et al.,* [14] provided an article with a detailed explanation of the different types of coiled fibers. Motojima *et al.,* [15] state that the structure's ability to resemble a carbon coil may lead to a variety of uses, such as absorbing materials. According to several authors [16, 17], carbon nanocoils produce materials that absorb electromagnetic waves more effectively than traditional ferrites.

The as-synthesised CNT can be used to reduce the intermolecular Van der Waals interactions between molecules by integrating it into an insulated polymer matrix. Since the MWCNT bundles generated irregularly shaped and sized aggregates and agglomerates in the epoxy matrix, the amount loaded was limited to 8wt%. Wang and Zhao [18] noted that, MWCNT loading of 8wt% may be optimal for the MWCNT-epoxy composite's microwave absorption since the microwave absorption of the sample with a 10wt% MWCNT loading did not significantly improve.

Figure 4(b) shows the well-separated and uniformly dispersion of CNT loaded into epoxy resin at magnification of 10 000. The enlarged view in Figure 4(c) at magnification of 50 000 showing closely part of the CNT dispersed in the epoxy resin. The composite samples formed a nearly linked network with tiny gaps between CNT ends. According to Qin and Brosseau [19], the interaction between inner electrons and exterior microwave radiation allows the individual CNTs and CNT bundles in the epoxy composite samples to absorb microwave energy and attenuate the radiation. Good dispersion improves the ability to absorb electromagnetic waves as reported by Che *et al.,* [20]. Indeed, precise and consistent EM wave absorption measurements are ensured by filler that is evenly distributed throughout the matrix. Zeng *et al.,* [21] reported that strong CNT-polymer interactions or enhanced compatibility of CNTs to the polymer matrix, which improve polymer-wrapping around CNTs, are good ways to reduce the electrical conductivity. Furthermore, compared to composites with uniformly dispersed CNTs, multi-walled carbon nanotube (MWCNT)/polymer composites containing CNT agglomerations at the microscale have been reported to have higher electrical conductivity as reported by Aguilar and Aviles [22]. The existence of both straight-like and twisted fiber is shown by the blue and red arrow respectively (Figure 4(a)). The presence of solid and hollow tube fiber is indicated by the blue and red circle respectively (Figure 4(b))

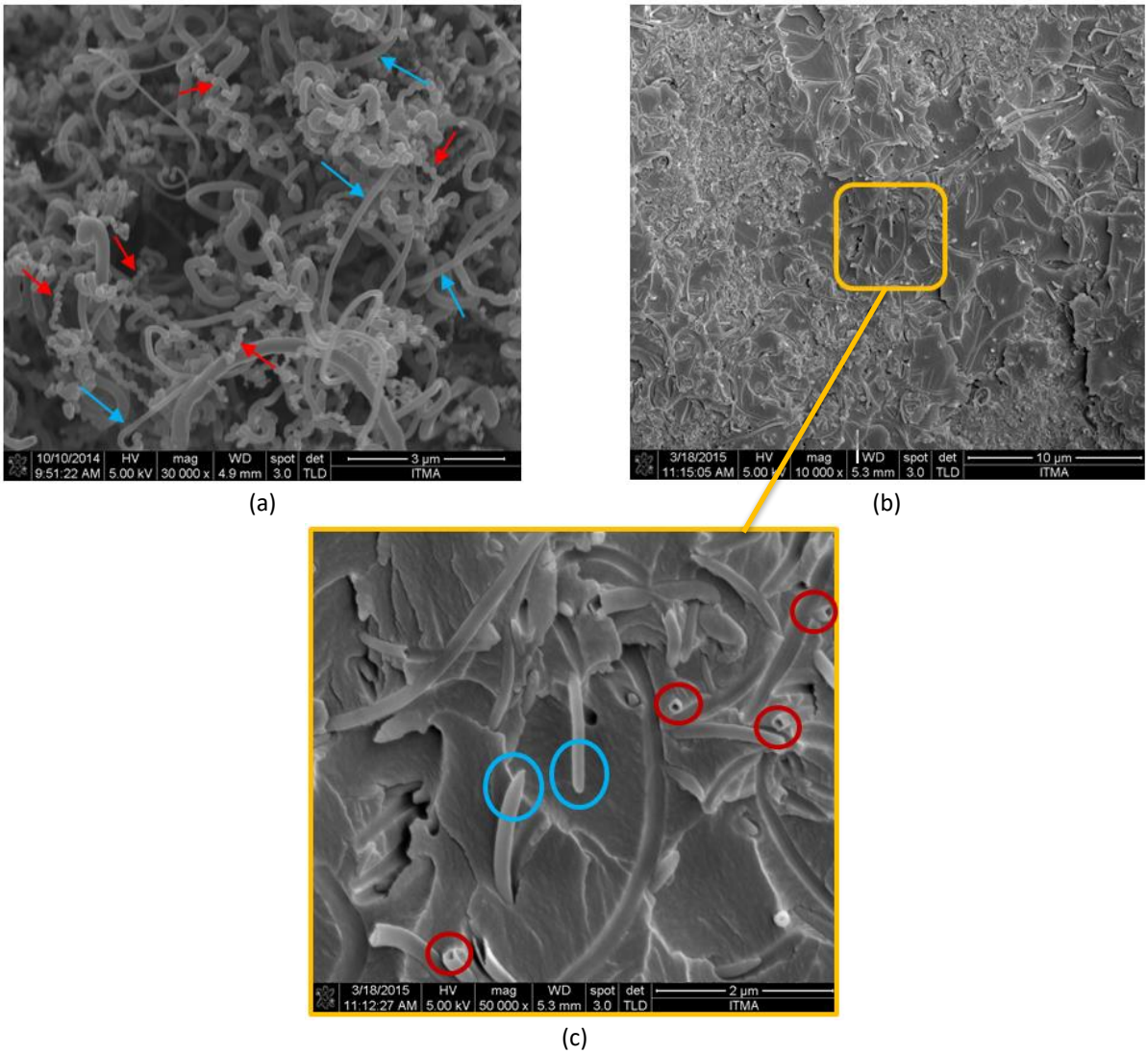

(a) (b)

(c)

Fig. 4. FESEM image of (a) synthesized carbon nanotubes by using S1 as catalysts, (b) CNT loaded into epoxy resin and (c) enlarged view of CNT loaded into epoxy resin

3.3 Structural Analysis

Table 1 shows the corresponding peak of more precise structural details about the carbon nanostructures in carbon nanocoils measured by using Raman scattering. The high value of D and G band intensities peak were observed at ~1350 cm^{-1} and ~1570 cm^{-1}, respectively. The G-peak is linked to the signal originating from the crystalline graphite, whereas the D-peak is indicative of the defects and disorder. Low graphitization of nanocoils is indicated by a large D-band peak and a broad G-band peak. For microwave absorption, low conductivity and appropriate dielectric loss are generally favorable. Therefore, reduced conductivity is correlated with a lower degree of graphitization. The intensity ratio of the D to G band, which is used to assess the quality of CNTs, is known to rely on the structural features of the CNTs. The ratios of these two peaks' intensities (I_D/I_G) ranged from 0.850 to 0.860, indicating either a reduced degree of graphitization or a defective structure in the resultant CNT. According to Cheng, *et al.,* [23], many defects have been caused and are attributed to tube end defects, staging disorders, and curved graphene layers. As a matter of fact, the existence of hollow structure may also be a factor and contributes to the formation of defects. Thus, it also contributes to the formation of multiwalled carbon nanotubes

compared to single walled carbon nanotubes that has higher degree of graphitization and sharp G peak.

Strong microwave absorption was contributed by the defects in the structure of carbon nanotubes (CNTs), which have been reported by authors [19] to function as polarization centers. Qin and Brosseau [19] also reported because MWCNTs were used to create the composite samples, their complex architectures resulted in more defects that improved microwave absorption that was primarily attributable to dielectric relaxation. Sufficient defects are important for microwave absorption since too many defects could give effect towards the microwave signal transmit through the materials.

Table 1
Peak frequencies of Raman spectra for synthesized CNT

Sample	**D-band (cm^{-1})**	**G-band (cm^{-1})**	**I_D/I_G**
CI	1352	1573	0.860
N	1350	1583	0.853
S1	1344	1577	0.852
S2	1348	1577	0.855
S3	1340	1569	0.854

3.4 Microwave Characterization

The reflection loss vs frequency graph as in Figure 5 was measured at frequency 8 – 12 GHz (X-band) and 12 - 18 GHz (Ku-band). The synthesised pure $Ni_{0.5}Zn_{0.5}Fe_2O_4$/P with thickness of 3 mm was discovered to have a reflection loss peak that emerged at a frequency lower than 8 GHz and had a reflection loss of -18 dB. However, because the reflection loss peak resonates at a much lower frequency range, it is not fully visible. In contrast, the reflection loss peak for was found to be at 8.5 GHz, with a reflection loss of -18 dB. As for thickness of 2mm, the reflection loss peak obtained for synthesised pure $Ni_{0.5}Zn_{0.5}Fe_2O_4$/P and synthesised carbonyl iron/P was -18 dB (15 GHz) and -16 dB (13.8 GHz) respectively. Since the reflection loss peak resonates at a significantly higher frequency range, it was not seen for thickness 1 mm for both as-synthesised $Ni_{0.5}Zn_{0.5}Fe_2O_4$/P and as-synthesised carbonyl iron/P. Table 2 showing another research being reported previously related to the materials.

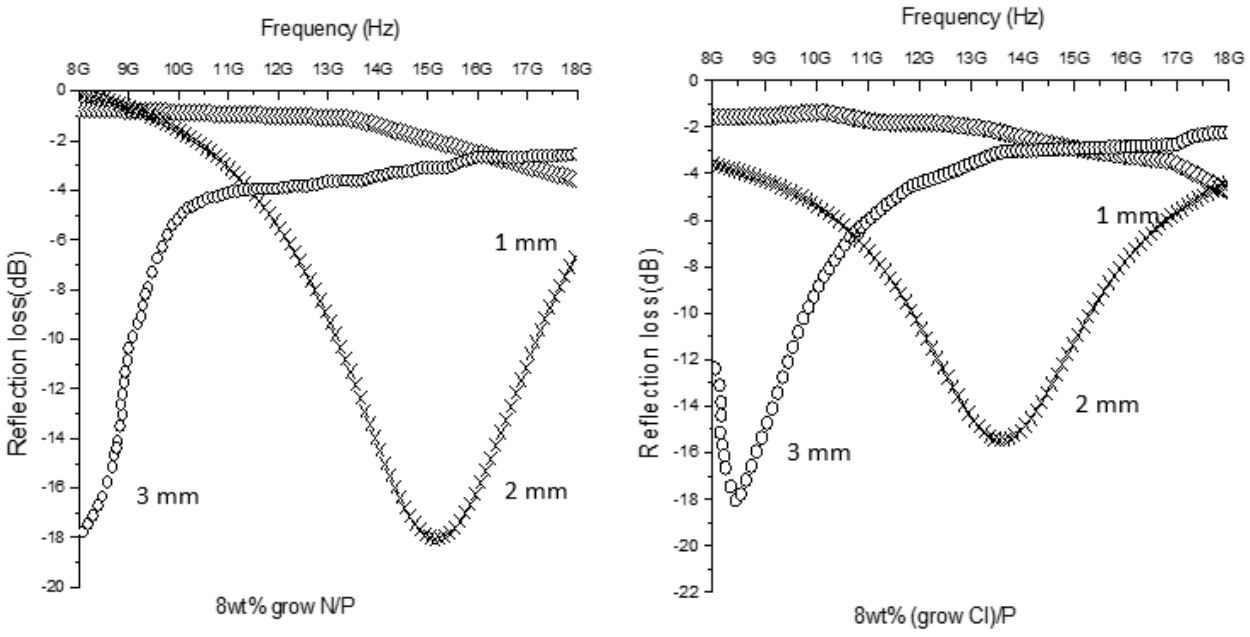

(a) (b)

Fig. 5. Reflection loss of synthesized CNT by using (a) N and (b) CI as catalyst at thickness of 1mm, 2mm and 3mm

Table 2
Reflection loss of different polymer composite material.

Composite material	Reflection loss (frequency)	Bandwidth (<-10 dB)	References
70wt% Pure CI/acrylic resin	-22.3 dB (13.5 GHz)	6 GHz (11-17 GHz)	[24]
50wt% CI/EPDM (Ethylene-propylene-diene monomer)	-11 dB (4 GHz, t= 1.1mm) -16 dB (11 GHz, t = 3.6 mm)	-	[25]
CI/epoxy resin (ratio 6:1)	-14 dB (3 GHz) -4 dB (15 GHz)	1 GHz	[26]
CI/CPE (chlorinated polyethylene)	-10 dB (10 GHz, t= 1mm)	-	[27]
8wt% CNT catalyzed by N/epoxy resin	-18 dB (15 GHz, t = 2mm)	4.5 GHz (13-17.5 GHz)	This work
8wt% CNT catalyzed by CI/epoxy resin	-16 dB (13.5 GHz, t= 2mm) -18 dB (8.5 GHz, t = 3 mm)	3.5 GHz (12-15.5 GHz) >1.5 GHz (<9.8 GHz)	This work
8wt% CNT catalyzed by S1/epoxy resin	-16 dB (~12.8 GHz, t= 2mm), -25 dB (~9.3 GHz, t=3mm),	3.8 GHz (11-14.8 GHz) 2.5 GHz (8 – 10.5 GHz)	This work
8wt% CNT catalyzed by S2/epoxy resin	-23 dB (~14.9 GHz, t=2mm), -26 dB (~9.4 GHz, t=3mm)	3.8 GHz (12.2-16 GHz) 2.5 GHz (8 – 10.5 GHz)	This work
8wt% CNT catalyzed by S3/epoxy resin	-13 dB (~15.1 GHz, t=2mm), -15 dB (~10.5 GHz, t=3mm)	3.5 GHz (13.5-17 GHz) 3.3 GHz (9.5-12.8 GHz)	This work

The reflection loss of thickness 1 mm (Figure 6(a)) showing that the microwave absorption peak start to form at higher frequency range (> 16 GHz). However, the reflection loss peak could not be fully observed since it resonates at much higher frequency range. On the other hand, sample of

thickness 2 mm (Figure 6(b)) showing clearly the reflection loss peak of -16 dB (~12.8 GHz), -23 dB (~14.9 GHz) and -13 dB (~15.1 GHz) for S1, S2 and S3 respectively. At thickness of 3 mm (Figure 6 (c)), the reflection loss peak observed was -25 dB (~9.3 GHz), -26 dB (~9.4 GHz) and -15 dB (~10.5 GHz) for S1, S2 and S3 respectively. Based on the result for all thicknesses, the reflection loss peak shifted slightly to the right as the mixture amount of $Ni_{0.5}Zn_{0.5}Fe_2O_4$ increased from 20% to 80% (S1 to S3). Regarding thickness 1 mm, the trend of moving to the right is still observable even though the reflection loss peak resonates at a significantly higher frequency. These may have occurred because of an increase in the fraction of $Ni_{0.5}Zn_{0.5}Fe_2O_4$ in the mixed ferrite as catalyst to synthesised CNT. The reflection loss value for all thicknesses showing dropped in the RL value as the amount of carbonyl iron for the synthesised CNT catalyzed by mixed ferrite reduced from 80% to 20% (S3 to S1).

The shift in matching frequency results in the reflection loss peak moves towards a lower frequency range as thickness increases.

For every polymer composite sample, the thickness of 2 mm provided the broad bandwidth. Broad bandwidth was defined as reflection loss values in all composite samples that were less than -10 dB. It should be noted that the frequency bandwidth with RL characteristics of over 90% was stated for the "10 dB absorbing bandwidth." The bandwidth with a reflection loss less than -10 dB is indicated by the dotted line (Figure 6). The bandwidth measured at -10 dB was also reported by Malhat *et al.,* [28]. Table 2 shows the bandwidth of the sample of thickness 2 and 3 mm.

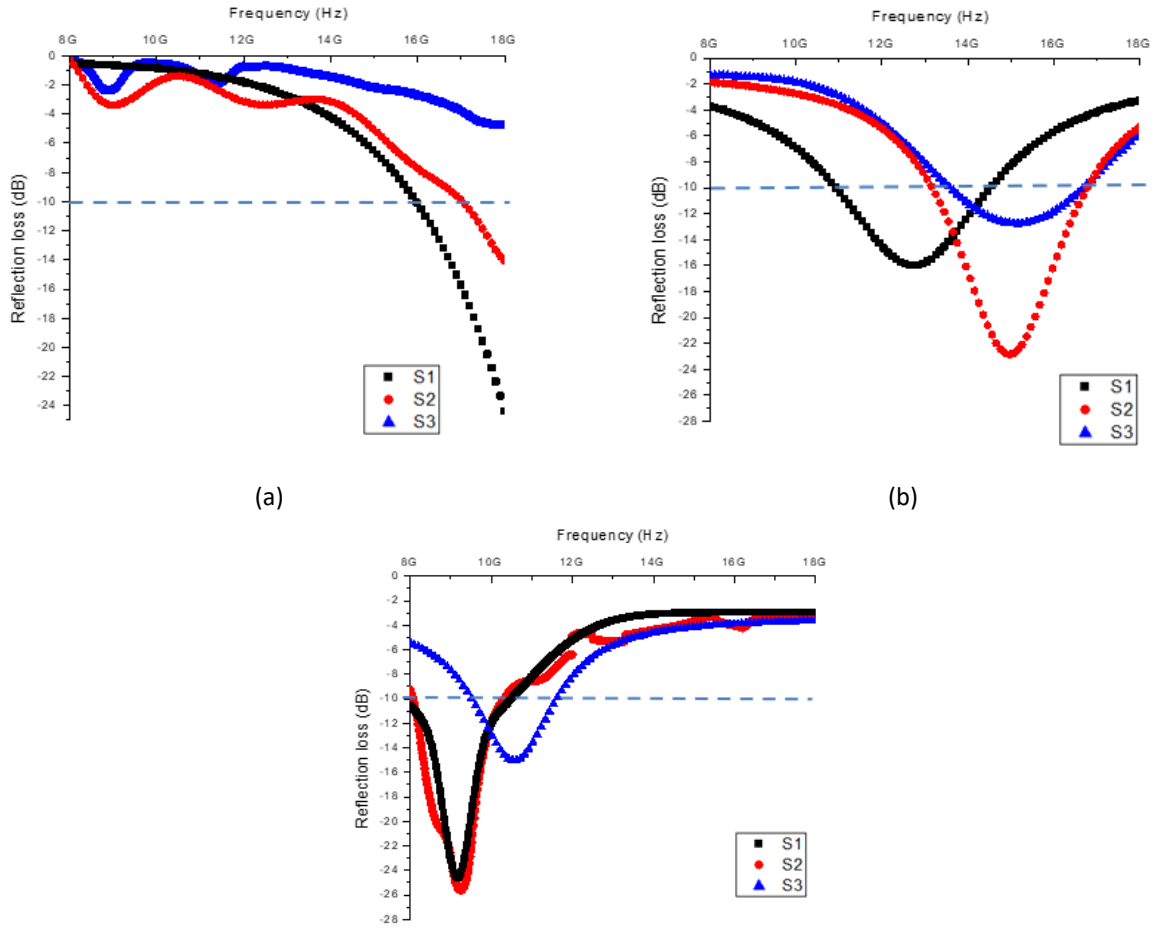

Fig. 6. Reflection loss of synthesized CNT by using S1, S2 and S3 as catalyst at thickness of (a) 1mm, (b) 2mm and (c) 3mm

4. Conclusions

In summary, ferrite mixed sample ($Ni_{0.5}Zn_{0.5}Fe_2O_4$ + Carbonyl Iron) used as catalyst to grow CNT with only 8wt% of synthesized CNT loaded into epoxy resin have better improvement in the reflection loss and absorb more compared to other single, mixed between two material or mixed with commercial CNT. The result show improvement in the value of reflection loss for the growth of mixed ferrite as increase the $Ni_{0.5}Zn_{0.5}Fe_2O_4$ content from 20% to 80% (S1 to S3). Microwave absorption was increased for as-synthesised CNT catalyzed by coupled $Ni_{0.5}Zn_{0.5}Fe_2O_4$ and Carbonyl iron loaded into epoxy matrix nanocomposites because there was greater impedance matching between the dielectric loss and magnetic loss. Through the interaction of inner electrons and external microwave radiation, the as-synthesised CNT in the epoxy composites contributes to the microwave absorption mechanism by absorbing the microwave energy and attenuating the radiation. Strong microwave absorption has been mostly associated with dielectric relaxation and polarization centres may potentially arise via the composite sample's defect development.

Acknowledgement
This research was funded by a grant from Ministry of Higher Education of Malaysia (Fundamental Research Grant Scheme (FRGS/1/2020/STG05/USIM/02/3) (USIM/FRGS/KGI/KPT/52020) and Long-Term Research Grant Scheme (LRGS/B-U/2013/UPNM/Defence & Security-P2).

References

[1] Pang, Huifang, Yuping Duan, Lingxi Huang, Lulu Song, Jia Liu, Tuo Zhang, Xuan Yang et al. "Research advances in composition, structure and mechanisms of microwave absorbing materials." Composites Part B: Engineering 224 (2021): 109173. https://doi.org/10.1016/j.compositesb.2021.109173

[2] Lu, Siru, Long Xia, Jiaming Xu, Chuheng Ding, Tiantian Li, Hua Yang, Bo Zhong et al. "Permittivity-regulating strategy enabling superior electromagnetic wave absorption of lithium aluminum silicate/rGO nanocomposites." ACS applied materials & interfaces 11, no. 20 (2019): 18626-18636. https://doi.org/10.1021/acsami.9b00348

[3] Mohamad, Noraiham, Anisah Abd Latiff, Jeefferie Abd Razak, Hairul Effendy Ab Maulod, Pay Jun Liew, Mohd Shahir Kasim, and Qumrul Ahsan. "Morphological Characteristics and Wear Mechanism of Recycled Carbon Fibre Prepreg reinforced Polypropylene Composites." Malaysian Journal on Composites Science and Manufacturing 5, no. 1 (2021): 1-10. https://doi.org/10.37934/mjcsm.5.1.110

[4] Idris, Fadzidah Mohd, Idza Riati Ibrahim, Farah Nabilah Shafiee, Hatika Kaco, and Mohd Shamsul Ezzad Shafie. "Materials' Properties of Lightweight Spiral Hybrid CNT/Epoxy Composites Enhanced Reflection Loss." *Journal of Advanced Research in Applied Mechanics* 113, no. 1 (2024): 13-26. https://doi.org/10.37934/aram.113.1.1326

[5] Gao, Huajing, Xinxin Zhao, Haimin Zhang, Jiafu Chen, Shifa Wang, and Hua Yang. "Construction of 2D/0D/2D face-to-face contact g-C 3 N 4@ Au@ $Bi_4Ti_3O_{12}$ heterojunction photocatalysts for degradation of rhodamine B." *Journal of Electronic Materials* 49 (2020): 5248-5259. https://doi.org/10.1007/s11664-020-08243-2

[6] Belin, Thomas, and Florence Epron. "Characterization methods of carbon nanotubes: a review." *Materials Science and Engineering: B* 119, no. 2 (2005): 105-118. https://doi.org/10.1016/j.mseb.2005.02.046

[7] Ryu, H., B. K. Singh, and K. S. Bartwal. "Synthesis and optimization of MWCNTs on Co-Ni/MgO by thermal CVD." *Advances in condensed matter physics* 2008 (2008). https://doi.org/10.1155/2008/971457

[8] Somiya, Shigeyuki. *Handbook of advanced ceramics: materials, applications, processing, and properties*. Academic press, 2013. https://doi.org/10.1016/B978-0-12-385469-8.03001-X

[9] Lambin, Ph, Annick Loiseau, Christine Culot, and L. P. Biro. "Structure of carbon nanotubes probed by local and global probes." *Carbon* 40, no. 10 (2002): 1635-1648. https://doi.org/10.1016/S0008-6223(02)00006-4

[10] Wang, Z., Hui, C. (2003) Electron microscopy of nanotube. Springer, Berlin. https://doi.org/10.1007/978-1-4615-0315-6

[11] Tessonnier, Jean-Philippe, Dirk Rosenthal, Thomas W. Hansen, Christian Hess, Manfred E. Schuster, Raoul Blume, Frank Girgsdies et al. "Analysis of the structure and chemical properties of some commercial carbon nanostructures." *Carbon* 47, no. 7 (2009): 1779-1798. https://doi.org/10.1016/j.carbon.2009.02.032

[12] McCaldin, S., M. Bououdina, D. M. Grant, and G. S. Walker. "The effect of processing conditions on carbon nanostructures formed on an iron-based catalyst." *Carbon* 44, no. 11 (2006): 2273-2280. https://doi.org/10.1016/j.carbon.2006.02.030
[13] Fejes, Dóra, and Klára Hernádi. "A review of the properties and CVD synthesis of coiled carbon nanotubes." *Materials* 3, no. 4 (2010): 2618-2642. https://doi.org/10.3390/ma3042618
[14] Hikita, Muneaki, Robyn L. Bradford, and Khalid Lafdi. "Growth and properties of carbon microcoils and nanocoils." *Crystals* 4, no. 4 (2014): 466-489. https://doi.org/10.3390/cryst4040466
[15] Motojima, S., S. Hoshiya, and Y. Hishikawa. "Electromagnetic wave absorption properties of carbon microcoils/PMMA composite beads in W bands." *Carbon* 41, no. 13 (2003): 2658-2660. https://doi.org/10.1016/S0008-6223(03)00292-6
[16] Zhao, Dong-Lin, and Zeng-Min Shen. "Preparation and microwave absorption properties of carbon nanocoils." *Materials Letters* 62, no. 21-22 (2008): 3704-3706. https://doi.org/10.1016/j.matlet.2008.04.032
[17] Tang, Nujiang, Wei Zhong, Chaktong Au, Yi Yang, Mangui Han, Kuanjiuh Lin, and Youwei Du. "Synthesis, microwave electromagnetic, and microwave absorption properties of twin carbon nanocoils." *The Journal of Physical Chemistry C* 112, no. 49 (2008): 19316-19323. https://doi.org/10.1021/jp808087n
[18] Wang, Z. and Guang, L. Z. "Microwave absorption properties of carbon nanotubes-epoxy composites in a frequency range of 2-20 GHz." Open Journal of Composite Materials 03(02)(2013):17-23. https://doi.org/10.1016/j.mseb.2010.07.007
[19] Qin, F., and Christian Brosseau. "A review and analysis of microwave absorption in polymer composites filled with carbonaceous particles." *Journal of applied physics* 111, no. 6 (2012). https://doi.org/10.1063/1.3688435
[20] Che, Bien Dong, Bao Quoc Nguyen, Le-Thu T. Nguyen, Ha Tran Nguyen, Viet Quoc Nguyen, Thang Van Le, and Nieu Huu Nguyen. "The impact of different multi-walled carbon nanotubes on the X-band microwave absorption of their epoxy nanocomposites." *Chemistry Central Journal* 9 (2015): 1-13. https://doi.org/10.1186/s13065-015-0087-2
[21] Zeng, You, Pengfei Liu, Jinhong Du, Long Zhao, Pulickel M. Ajayan, and Hui-Ming Cheng. "Increasing the electrical conductivity of carbon nanotube/polymer composites by using weak nanotube–polymer interactions." *Carbon* 48, no. 12 (2010): 3551-3558. https://doi.org/10.1016/j.carbon.2010.05.053
[22] Aguilar, J. O., J. R. Bautista-Quijano, and F. J. E. P. L. Avilés. "Influence of carbon nanotube clustering on the electrical conductivity of polymer composite films." *Express Polym Lett* 4, no. 5 (2010): 292-299. https://doi.org/10.3144/expresspolymlett.2010.37
[23] Cheng, Jipeng, Xiaobin Zhang, Zhiqiang Luo, Fu Liu, Ying Ye, Wanzhong Yin, Wei Liu, and Yuexin Han. "Carbon nanotube synthesis and parametric study using CaCO3 nanocrystals as catalyst support by CVD." *Materials chemistry and physics* 95, no. 1 (2006): 5-11. https://doi.org/10.1016/j.matchemphys.2005.04.043
[24] Li, Yong, Changxin Chen, Xiaoyan Pan, Yuwei Ni, Song Zhang, Jie Huang, Da Chen, and Yafei Zhang. "Multiband microwave absorption films based on defective multiwalled carbon nanotubes added carbonyl iron/acrylic resin." *Physica B: Condensed Matter* 404, no. 8-11 (2009): 1343-1346. https://doi.org/10.1016/j.physb.2008.12.015
[25] Feng, Y. B., T. Qiu, and C. Y. Shen. "Absorbing properties and structural design of microwave absorbers based on carbonyl iron and barium ferrite." *Journal of Magnetism and magnetic materials* 318, no. 1-2 (2007): 8-13. https://doi.org/10.1016/j.jmmm.2007.04.012
[26] Chen, Liyang, Yuping Duan, Lidong Liu, Jingbo Guo, and Shunhua Liu. "Influence of SiO2 fillers on microwave absorption properties of carbonyl iron/carbon black double-layer coatings." *Materials & design* 32, no. 2 (2011): 570-574. https://doi.org/10.1016/j.matdes.2010.08.021
[27] Liu, Lidong, Yuping Duan, Shunhua Liu, Liyang Chen, and Jingbo Guo. "Microwave absorption properties of one thin sheet employing carbonyl–iron powder and chlorinated polyethylene." *Journal of Magnetism and Magnetic Materials* 322, no. 13 (2010): 1736-1740. https://doi.org/10.1016/j.jmmm.2009.12.017
[28] Malhat, H. A., S. Abdelhamied, and S. H. Zainud-Deen. "High Gain and Radiation Efficiency Rectangular on-Chip Microstrip Patch Antenna for 60 GHz Applications." *Journal of Advanced Research in Applied Mechanics* 41, no. 1 (2018): 16-21.